Formation of Naphthalene, Indene, and Benzene from Cyclopentadiene Pyrolysis: A DFT Study

Dong Wang[†] and Angela Violi*

Department of Mechanical Engineering, University of Michigan, Ann Arbor, Michigan 48109

Do Hyong Kim and James A. Mullholland

Department of Civil and Environmental Engineering, Georgia Institute of Technology, Atlanta, Georgia 30332-0512

Received: July 3, 2005; In Final Form: January 25, 2006

Four new reaction pathways for polycyclic aromatic hydrocarbon growth from cyclopentadiene pyrolysis are proposed and investigated using the B3LYP/6-31G(d,p) level of theory. These pathways allow for the production of indene, naphthalene, and benzene through intramolecular addition, C−H β-scission, and C−C β-scission reaction mechanisms, respectively. Results show that the intramolecular addition channel is favored at low temperatures, and the C−H β-scission channel and the newly identified C−C β-scission pathway become significant when the temperature increases. These results are in qualitative agreement with the experimental results previously obtained by this research group indicating that the main product at low temperature is indene, while benzene and naphthalene production dominate at the high-temperature end.

1. Introduction

Polycyclic aromatic hydrocarbons (PAH) are important combustion-generated pollutants, both because of their role as potential soot precursors[1,2] and because of the inherent biological activity of particular PAH.[3,4] Despite significant progress in understanding single processes, the comprehensive theory and models that predict the formation of PAH fall short of predicting many of the experimental observations.

The seminal work in this area is due to Frenklach and co-workers,[5−8] who developed a model for PAH formation in which the molecular mass growth occurs by way of a two-step process involving hydrogen abstraction to activate the aromatic molecule followed by subsequent acetylene addition. Cyclization to the next higher order ring occurs when the sequence H abstraction followed by acetylene addition is repeated (HACA mechanism). However, the aromatic growth can proceed through different routes, and many other species have been proposed as potential precursors such as methyl, propargyl, and cyclopentadienyl.[9−16] In particular, the importance of cyclopentadienyl (CPDyl) moieties in PAH growth has been postulated because these radicals are neutral and ambident−reactive at different sites. Fuels containing cyclopentadienyl moieties have also shown high sooting tendencies.[17] In addition, relative to other aromatics, PAH with peripherally fused five-membered rings (CP-PAH) demonstrate a greater facility in undergoing certain kinds of reactions, such as isomerization involving intramolecular rearrangement.[18,19] This is due to the fact that fusion of the cyclopenta ring alters the electronic properties of PAH, as demonstrated by differences in resonance energy[20] and measured differences[21] in ultraviolet−visible (UV) absorption and fluorescence.

To study the importance of CPDyl moieties in PAH growth, Mulholland and co-workers have conducted a detailed experimental analysis of CP-PAH growth[22,23] in a laminar flow reactor. In particular, for the pyrolysis of cyclopentadiene, benzene, indene, and naphthalene were identified as major products.[24] One of the species identified (naphthalene) can be formed by reactions analogous to those in the radical−radical mechanism proposed by Melius et al.,[9] which describes the conversion of two CPDyl radicals to naphthalene, but other observed products are instead more likely produced through a previously unknown radical−molecule pathway. Therefore, it is necessary to carry out a thorough analysis of the CPD pyrolysis system.

The importance of radical−molecule reactions for the growth of PAH and high molecular mass compounds has also been investigated by Violi and co-workers[25−27] who have proposed a sequence of radical−molecule reactions between aromatic compounds with six π-electrons and compounds containing conjugated double bonds (e.g., acenaphthylene) to explain the formation of PAH and higher molecular mass compounds in flames. Through a two-step radical−molecule addition reaction followed by rearrangement of the carbon framework, this mechanism leads to the formation of high molecular mass compounds frequently found in flames. The distinguishing features of this model lie in the chemical specificity of the routes considered, where the aromatic radical attacks the double bond of the five-membered ring PAH. This involves specific compounds that form resonantly stabilized radical intermediates, relieving part of the large strain in the five-membered rings by formation of linear aggregates.

In this paper, we apply this radical−molecule model to the construction of new reaction pathways for the formation of benzene, indene, and naphthalene from the pyrolysis of CPD. In particular, the density functional theory (DFT) is employed to determine the energetics of the system, to assess the viability of the new pathways, and for comparison to the mechanism

* Corresponding author. Phone: (734) 615-6448. E-mail: avioli@umich.edu.

[†] Present address: Department of Chemistry, University of Utah, Salt Lake City, UT 84112.

10.1021/jp053628a CCC: $33.50
Published on Web 03/21/2006

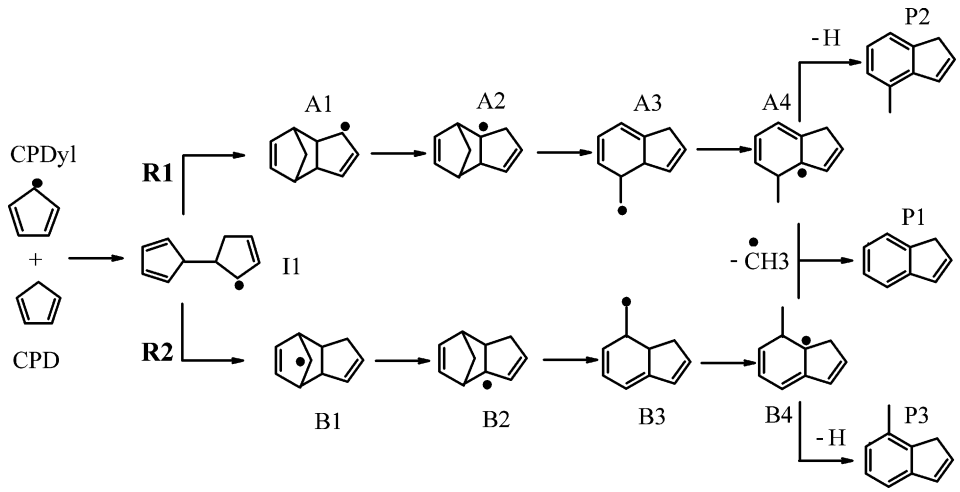

Figure 1. Intramolecular addition pathways R1 and R2 to indene.

proposed by Melius. We also use these results to make a qualitative comparison to experimental data,[24] in order to verify that our radical−molecule approach is appropriate.

2. Computational Details

Geometries and frequencies of the reactants, transition states, and products in the system CPD−CPDyl were calculated by using the hybrid density functional B3LYP method (i.e., Becke's three-parameter nonlocal exchange functional[28] with the nonlocal correlation function of Lee, Yang, and Parr[29,30]), with the 6-31G(d,p) basis set.

Transition-state (TS) geometries are identified by the existence of only one imaginary frequency in the normal mode coordinate analysis, an evaluation of the TS geometry, and the reaction coordinate's vibrational motion. The frequency calculations also allow the zero-point energy (ZPE) corrections to be obtained. In case of transition structures, the movement of atoms in the imaginary frequency mode can be displayed to see if the atoms are moving in the right direction toward the reactant and product. IRC (intrinsic reaction coordinate) calculations were carried out to guarantee that the transition states found indeed connect the reactant and product of the reaction step. All calculations were done by using the Gaussian 03 program.[31]

Comprehensive studies of neutral and cationic PAH containing six-membered rings using the B3LYP/6-31G(d,p) level of theory have been shown to be able to predict the vibrational frequencies and the relative intensities with good accuracy.[32]

Unimolecular reactions of the chemically activated and stabilized adducts resulting from addition or combination reactions are analyzed by first constructing potential energy diagrams for the reaction system. DFT calculations are used to calculate transition-state structures and activation energies for isomerization, β-scission, and dissociation reactions. The enthalpies and entropies are treated with conventional transition-state theory to calculate Arrhenius preexponential factors and energies of activation that result in high-pressure-limit rate constants ($k\infty$) as functions of temperature. Nonlinear Arrhenius effects resulting from changes in the thermochemical properties of the respective transition state relative to those of its adduct with temperature are incorporated using a two-parameter Arrhenius preexponential factor (A, n) in AT^n. Rate constants of the first reaction steps of each pathway were calculated from the transition-state theory (TST), using TheRate code (THEoretical RATEs)[33] at the CSEO online resource (http://www.cseo.net). The transmission coefficients which account for the quantum mechanical tunneling effect were calculated using the Eckart method.[34]

The thermal rate coefficient is expressed as

$$k(T) = \kappa(T)\sigma\frac{k_B T}{h}\frac{Q^{\ddagger}(T)}{\Phi^{R}(T)}e^{-\Delta V^{\ddagger}/k_B T}$$

where κ is the transmission coefficient accounting for the quantum mechanical tunneling effects, σ is the reaction symmetry number, $Q^{\ddagger}$ and Φ^{R} are the total partition functions (per unit volume) of the transition state and reactant, respectively, $\Delta V^{\ddagger}$ is the classical barrier height, T is the temperature, and k_B and h are the Boltzmann and Planck constants, respectively.

3. Results

The reaction mechanism for the formation of naphthalene combining two CPDyl radicals has been already investigated by Melius et al.,[9] and results have been reported using the bond additivity-corrected fourth-order perturbation Møller−Plesset (BAC-MP4) and BAC-MP2 levels of theory. To compare the feasibility of different reaction pathways, below we reported results for the Melius mechanism (C−H bond β-scission) using the B3LYP method together with newly identified reaction pathways.

Intramolecular Reactions. Figure 1 shows the reaction pathways for the addition of CPD to CPDyl to produce indene (pathways R1 and R2). The reaction of CPD with CPDyl begins with the addition of the cyclopentadienyl radical to the π-bond of CPD to produce a resonantly stabilized CPD−CPDyl dimer (I1). The intermolecular addition barrier is 11.5 kcal/mol. From I1, a bridged intermediate is produced with the radical either on C-1 (A1) or on the bridged atom (B1). The energy barrier for the formation of A1 is 17.85 kcal/mol, much lower than the energy required to produce B1 that is 32.06 kcal/mol. Intermediates A2 and B2 with the radicals on C-7a and C-3a, respectively, are then obtained through hydrogen migration reactions. The subsequent bridge-opening step produces bicyclical intermediates with the radical on the methyl group (A3 and B3). The energy barriers for the formation of A3 (37.9 kcal/mol) and B3 (38.2 kcal/mol) are similar. A3 and B3 undergo further 1,3-H shift to produce A4 (the radical is on C-3a) and B4 (the radical is on C-7a). The loss of the methyl group produces indene (P1). The energy barriers for A4 → P1 + CH_3 and B4 → P1 + CH_3 are 22 and 19.7 kcal/mol, respectively.

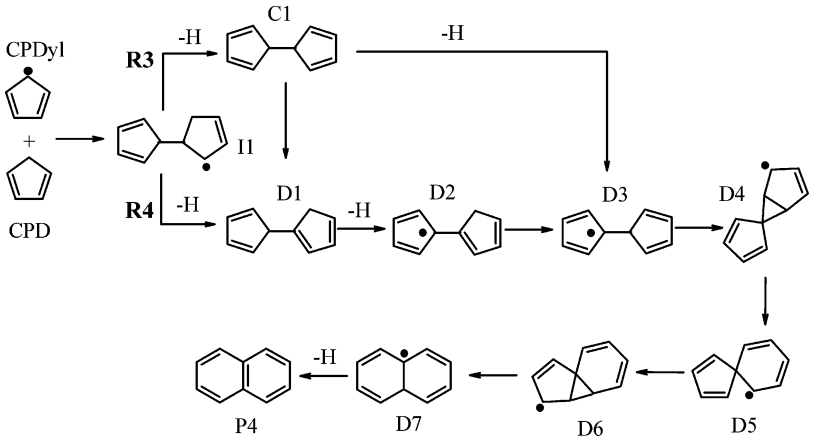

Figure 2. C−H bond β-scission pathways R3 and R4 to naphthalene.

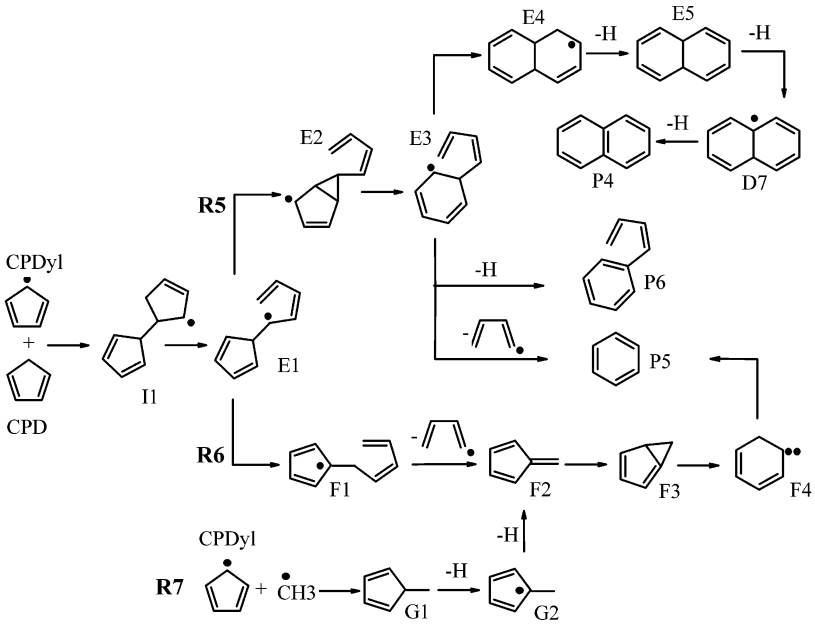

Figure 3. C−C bond β-scission pathways R5 and R6 to naphthalene and benzene.

As an alternative, A4 can undergo H elimination to form 4-methyl indene (P2), and in a similar way B4 produces 7-methyl indene (P3).

C−H Bond β-Scission. Figure 2 shows the C−H bond β-scission pathways R3 and R4 that lead to the formation of naphthalene. Through H elimination, I1 forms 9,10-dihydrofulvalene (C1), which rearranges to form the more stable 1,10-dihydrofulvalene (D1). The energy barriers for I1 → C1 + H and C1 → D1 are 48.45 and 24.06 kcal/mol, respectively. The loss of a H atom from the 10-carbon site of D1 produces a resonance-stabilized radical D2, and its isomerization by 1,3-H shift leads to D3, which can also be formed by eliminating a H atom directly from C1. D3 undergoes three-membered ring closure (D4) and subsequent opening to complete the ring expansion (D5). At the B3LYP/6-31G(d,p) level, the activation energy for the reaction D3 → D4 is 12.4 kcal/mol while the reaction D4 → D5 has an energy barrier of 23.2 kcal/mol. This process can be repeated, converting a second five-membered ring to a six-membered ring. A final C−H bond β-scission yields naphthalene and a H atom.

C−C Bond β-Scission. Competing with the above-mentioned pathways, new reaction pathways are proposed that involve the β-scission of a C−C bond. Figure 3 reports the various steps for pathways R5 and R6. Pathway R5 leads to the formation of either naphthalene or benzene, while pathway R6 shows the reaction sequence for the production of benzene. The molecule−radical dimer I1 undergoes a β-scission of the C−C bond, opening one of the two five-membered rings, to form intermediate E1. The energy barrier required for this step is 41.21 kcal/mol. The other five-membered ring expands to a six-membered ring via a three-membered ring closure step to form E2 first and then E3. The barriers for the reactions E1 → E2 and E2 → E3 are 15.3 and 19.6 kcal/mol, respectively. At this point intermediate E3 can either undergo another C−C bond β-scission to form benzene and butadienyl, or through further cyclization it can form two fused six-membered rings (E4). The initial loss of H from C-1 forms 9,10-dihydronaphthalene. Naphthalene (P4) is then produced by H elimination from the two fusing C atoms. From *cis*-9,10-dihydronaphthalene, two H atoms can also be eliminated simultaneously as H_2, and in this case the computed energy barrier is 75.53 kcal/mol. The energy values presented in Table 1 and Figure 7 below are for the trans structures only.

Pathway R6, on the other hand, forms benzene through the isomerization of fulvene. The initial C−C β-scission step from I1 to E1 is the same as in pathway R5. Instead of undergoing a three-membered ring closure as in pathway R5, E1 rearranges itself to form intermediate F1 through H atom shift. The

TABLE 1: Energy Barrier for Each Step of the Reaction at the B3LYP/6-31G(d,p) Level

reactions[a]	forward (kcal/mol)	reverse (kcal/mol)
CPD + CPDyl = I1	11.48	20.19
I1 = A1	17.85	17.86
A1 = A2	52.29	36.53
A2 = A3	37.93	41.98
A3 = A4	25.27	63.10
A4 = P1 + CH_3	22.00	10.63
A4 = P2 + H	28.27	4.35
I1 = B1	32.06	9.83
B1 = B2	42.33	57.44
B2 = B3	38.19	40.36
B3 = B4	29.06	56.70
B4 = P1 + CH_3	19.65	12.23
B4 = P3 + H	24.95	4.79
I1 = C1 + H	48.45	0.58
C1 = D1	24.06	27.32
C1 = D3 + H	72.87[b]	
I1 = D1 + H	45.13	0.52
D1 = D2 + H	58.80[b]	
D2 = D3	34.99	17.66
D3 = D4	12.38	2.35
D4 = D5	23.22	38.18
D5 = D6	13.10	5.94
D6 = D7	11.74	36.10
D7 = P4 + H	14.69	9.29
I1 = E1	41.21	32.40
E1 = E2	15.25	4.07
E2 = E3	19.56	37.75
E3 = P5 + C_4H_5	24.32	7.23
E3 = P6 + H	26.65	6.91
E3 = E4	28.24	37.75
E4 = E5 + H	51.48	0.52
E5 = D7 + H	55.36[b]	
E1 = F1	30.32	33.03
F1 = F2 + C_4H_5	47.71	0.56
F2 = F3	42.38	−0.27
F3 = F4	27.44	14.47
F4 = P5	1.82	91.80
CPDyl + CH_3 = G1	−63.06[b]	
G1 = G2 + H	73.06[b]	
G2 = F2 + H	54.14[b]	

[a] P1, indene; P2, 4-methyl indene; P3, 7-methyl indene; P4, naphthalene; P5, benzene; F2, fulvene; C1, 9,10-dihydrofulvalene; D1, 1,10-dihydrofulvalene; E5, 9,10-dihydronaphthalene; P6, phenyl-butadiene. [b] No transition state found, energy difference between reactant and product.

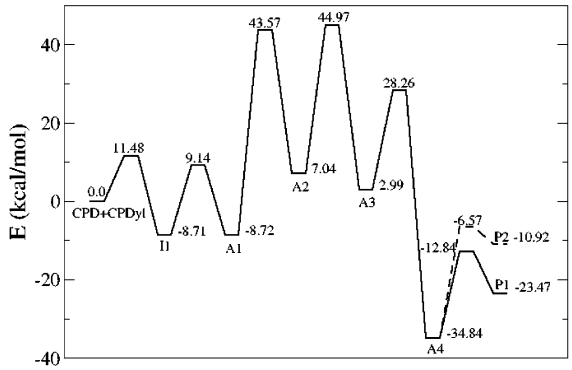

Figure 4. Potential energy diagram for pathway R1.

following β-scission of the C−C bond produces fulvene (F2) and butadienyl radical. Fulvene forms isofulvene (F3) with a five-membered ring and a three-membered ring fused together. Cyclohexadiene carbene (F4) is formed with an energy barrier of 27.4 kcal/mol, and it then undergoes hydrogen migration to produce benzene.

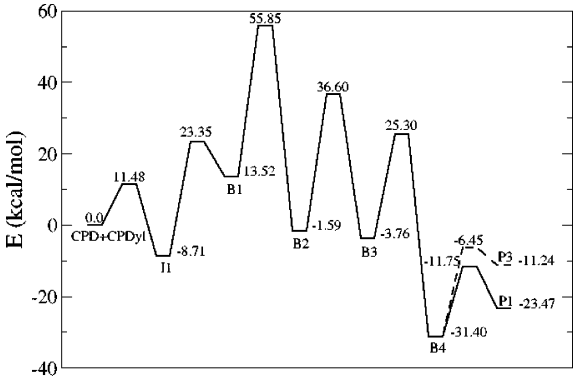

Figure 5. Potential energy diagram for pathway R2.

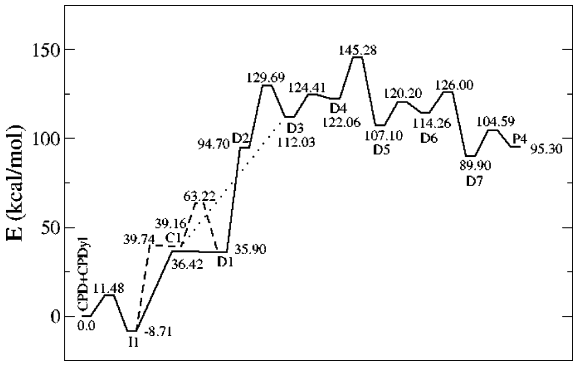

Figure 6. Potential energy diagrams for pathways R3 and R4.

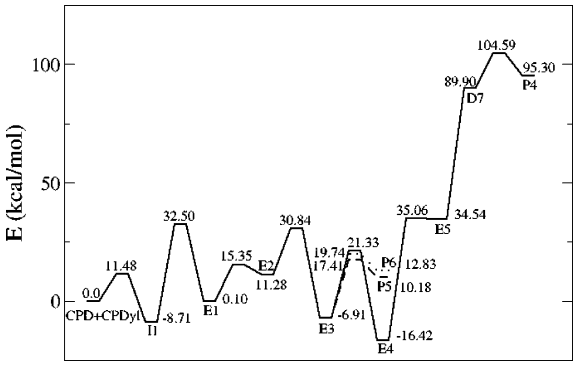

Figure 7. Potential energy diagram for pathway R5.

The potential energy surface for the thermal isomerization of fulvene to benzene was studied by Melius et al.[35] using the BAC-MP4 method and Madden et al.[36] using the modified Gaussian-2 (G2M) method. The activation energy was calculated to be 73.2 and 74.3 kcal/mol, respectively, which is 5−9 kcal/mol and 6−10 kcal/mol higher in energy than that obtained by Gaynor et al.[37] in their brief very low-pressure pyrolysis (VLPP) experiments. Similar results were obtained by Miller and Klippenstein[38] using a combination of QCISD(T) and MP2 methods. Therefore, the more sophisticated methods of calculation did not find significant differences in the activation energy for the isomerization reaction. The pathway presented here is similar to the multistep mechanism introduced by Madden et al.,[36] except that we identified two transition structures in the reaction step from F3 to F4. One of the two structures corresponds to the transition state reported by Madden et al. (labeled as TS2 in ref 36) while the other is 4.4 kcal/mol lower in energy at the B3LYP/6-31G(d,p) level of theory. By using the latter transition structure, the highest barrier we obtained is 70.1 kcal/mol. Details regarding this new transition state are reported in the Supporting Information.

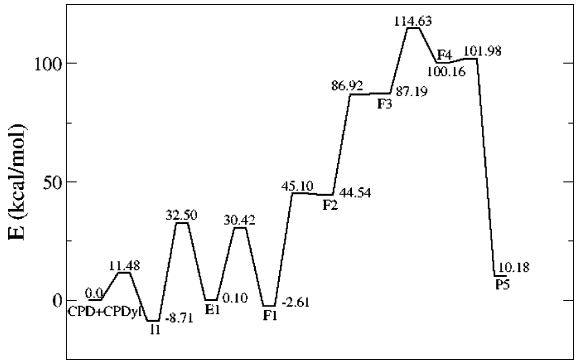

Figure 8. Potential energy diagram for pathway R6.

Merz and Scott[39] also investigated this multistep pathway in their study of the thermal automerization of benzene. The bicyclic intermediate isofulvene on the pathway from fulvene to carbene disappeared when the thermodynamic corrections were taken into account, which was also seen in our calculations.

In addition to pathway R6, fulvene can also be formed by combining CPDyl radical with the methyl radical produced in pathways R1 and R2, and then eliminating two hydrogen atoms. This reaction sequence is reported in Figure 3 as route R7.

The potential energy surface diagrams for the reaction pathways R1−R6 are reported in Figures 4−8. The values shown in the figures are inclusive of the zero-point energies $E = E_{elec} + ZPE$. Table 1 lists the energy barriers (ΔE) for the forward and reverse reactions of all the steps previously described. It is worth noticing that not all the reactions listed in Table 1 have a transition structure. For instance, no transition state has been found in the C1 = D3 + H, D1 = D2 + H, E5 = D7 + H reaction steps and steps in pathway R7. The above-mentioned reactions have something in common: they are essentially reactions between radicals or a radical and a hydrogen atom. In some cases, the transition structures are very close to either the reactant or the product geometrically and energetically, indicating that there exists a very shallow well in the potential energy surface.

The B3LYP method gives good estimations of the reaction energies, but it underpredicts the energetic barriers by 4−5 kcal/mol, and more accurate methods can be used in the future, such as BH&HLYP/6-31G(d,p).[40] The BH&HLYP method predicts rather accurate barrier heights, particularly for hydrogen abstraction reactions by a radical in comparison with those of more expensive calculations.[41]

4. Discussion

An important result obtained in this study is the identification of additional energetically favored pathways for the formation of naphthalene and benzene via C−C bond β-scission. The barrier from I1 to E1 (R5 and R6) is lower than the one from I1 to C1 + H or D1 + H (R3 and R4), being 41.21 kcal/mol for the C−C bond β-scission reactions because of relatively weak C−C bond compared with 48.45 and 45.13 kcal/mol for the cleavage of the C−H bond in pathways R3 and R4.

The computational results reported above are in qualitative agreement with the experimental observations on CPD pyrolysis.[24] The PAH products from dicyclopentadiene (DCPD) pyrolysis at 550−850 °C were numerous. Some of the identified products are formed through reactions similar to the one reported in the radical−radical mechanism of Melius et al.[9] for the conversion of two CPDyl radicals to naphthalene, but other observed products are instead more likely produced through different mechanisms.[24]

The major products from CPD pyrolysis were benzene, indene, and naphthalene. The formation of benzene and indene supports the existence of radical−molecule pathways[22,23] in addition to radical−radical pathways producing naphthalene.[9] The mechanisms reported in Figures 1−3 show radical−molecule pathways that can be invoked to explain the experimental evidences. Experimentally, the amount of indene produced exceeds that of naphthalene and benzene at low temperatures, and then the concentration profile of indene starts to decrease at 750 °C where naphthalene represents the major product. The computed pathways R1 and R2 have the lowest energy barriers among the various reaction channels, so it is reasonable to assume that indene will be the major compound produced at low temperatures. Between the intramolecular additions that lead to indene, pathway R1 is apparently more favorable since the energy barrier is 17.85 kcal/mol from I1 to A1, compared with the 32.06 kcal/mol required for the transition from I1 to B1. As the temperature increases, the C−H bond β-scission and the C−C bond β-scission pathways become significant. As a result naphthalene and benzene are produced.

In addition to these major products, $C_{10}H_{10}$ compounds such as methyl indene, dihydrofulvalene, and dihydronaphthalene were also observed in the experiment. The existence of these compounds further confirms the intramolecular addition, C−H bond β-scission, and C−C bond β-scission pathways identified on the basis of quantum mechanical computations. Experimentally, an unidentified $C_{10}H_{10}$ compound was reported, and its mass spectrum excluded the possibility of being dihydrofulvalene. As shown in Figure 3 (pathway R5), intermediate E3 can either undergo a C−C bond β-scission to form benzene and butadienyl, or eliminate a hydrogen atom to produce phenyl-butadiene ($C_{10}H_{10}$) with the energy barrier being 26.65 kcal/mol for the latter. We suspect that the unknown $C_{10}H_{10}$ compound detected in the experiment might be phenyl-butadiene.

Other aromatic products experimentally observed include toluene, styrene, fluorene, phenanthrene, and anthracene, which can be formed through reactions with smaller aromatic products. As soon as benzene is formed it can undergo H abstraction to produce C_6H_5 radical[42] that can react with the CH_3 radical produced from pathways R1 and R2 to form toluene.[43−46] In the same way, once indene is formed it can react with the CPDyl radical to produce fluorene, phenanthrene, and anthracene.[23,47]

All of the pathways described above share the same initial step that consists of the addition of cyclopentadienyl radical to the π-bond of cyclopentadiene CPD + CPDyl → I1. The second step differentiates the pathways analyzed. Rate constants for the second step of pathways R1−R5 are calculated using the transition-state theory (TST) and are listed in Table 2 in the form of Arrhenius parameters. At low temperatures the intramolecular addition pathways R1 and R2 are dominant, which is in agreement with the experimental results that the yield of indene is larger than that of naphthalene and benzene at temperatures lower than 750 °C. As the temperature increases, the entropy contribution becomes significant, and the C−C bond β-scission and C−H bond β-scission rates increase quicker than the intramolecular addition rate. The temperature-dependent pattern of rate constants suggests that the C−C bond and C−H bond β-scission pathways are entropically favorable.

The H elimination steps in the pathways proposed above are considered to occur through unimolecular β-scission reactions, but in a hydrogen-rich environment bimolecular H abstraction reactions need to be considered too. For the systems studied in this paper, it is possible to identify two classes of H elimination reactions: (a) the unpaired electron left on the carbon is

TABLE 2: Arrhenius Parameters for the First Two Reaction Steps of Pathways R1−R5[a]

	forward			reverse		
reactions	A	n	E_a (kcal/mol)	A	n	E_a (kcal/mol)
CPD + CPDyl= I1	3.55	2.75	9.90	1.58×10^{12}	0.48	20.5
I1 = A1	10.8×10^{10}	0.10	17.2	1.74×10^{12}	0.44	18.2
I1 = B1	13.3×10^{10}	0.06	31.4	1.54×10^{12}	0.38	10.0
I1 = C1 + H	1.22×10^{10}	1.16	48.7	6.90×10^{8}	1.44	−0.125
I1 = D1 + H	1.55×10^{10}	1.16	45.5	3.99×10^{8}	1.43	−0.264
I1 = E1	50.3×10^{10}	0.71	41.5	1.23×10^{11}	0.39	32.0

[a] The units of the rate constants $k(T) = A(T^n) \exp(-E_a/RT)$ are s^{-1} for monomolecular reactions and $cm^3\ mol^{-1}\ s^{-1}$ for bimolecular reactions, respectively.

delocalized to form a resonantly stabilized free radical, and (b) a conjugated double bond with other π-electrons is formed, which significantly stabilizes the system.

For the class a, the first reaction calculated is $C_5H_6 + H = C_5H_5 + H_2$ with the energy barrier being only 1.18 kcal/mol, which is much lower than the energy required for H elimination being 78.6 kcal/mol. The low barrier is attributed to the fact that the hydrogen to be removed was bonded to a saturated carbon atom, in comparison with the barrier being 10−20 kcal/mol[40] for the hydrogen abstraction from an unsaturated double-bonded carbon in PAH.

Similarly, reaction C1 + H = D3 + H_2 has a barrier of 0.18, and that of G1+ H = G2 + H_2 is 0.16 kcal/mol. The transition state has been located for the reactions D1 + H = D2 + H_2 and E5 (*cis*-9,10-dihydronaphthalene) + H = D7 + H_2 with the energy 0.25 and 0.39 kcal/mol lower than the reactant after ZPE correction, indicating that loss of H from these species happens fast in a hydrogen-rich environment. Class b includes the H abstraction from a saturated carbon of a resonantly stabilized radical to form more stable conjugated double-bond structure. Reactions I1 + H = C1 (or D1) + H_2, D7 + H = P4 + H_2, E4 + H = E5 + H_2, G2 + H = F2+ H_2 follow in this category, and no transition state has been identified for these reactions at the level of theory employed.

The low-energy barrier identified for the first class of H abstraction reactions and other supporting evidences in the literature, however, give us great confidence that the reactions in both cases happen rapidly; for example, reaction *i*-C_4H_3 + H = C_4H_2 + H_2 (R182, Table 1)[48] has zero activation energy; no transition state was found for abstraction of H from the phenyl and acenaphthylene adduct at the B3LYP/6-31G(d,p) level.[26] As mentioned before, the B3LYP/6-31G(d,p) level of theory is inadequate for hydrogen abstraction reactions by radicals, while BH&HLYP performs much better in this regard.[40,41]

Since the H elimination steps are mostly involved in the pathways leading to naphthalene, in a hydrogen-rich environment the formation rate of naphthalene will be greatly improved. The experiment shows that naphthalene yield is greater than indene above 1000 K, while the rate constant calculation for the branching step shows that the crossover is at 2000 K. This discrepancy might be explained by including H abstraction reactions.

Another explanation for the discrepancy between experimental and computed kinetic results on the temperature at which the naphthalene yield becomes greater than the indene yield is that the radical−radical pathway of naphthalene formation is competitive with the radical−molecule pathway. The formation of benzene and indene supports the existence of the CPD−CPDyl addition pathway, while naphthalene can be formed by either the CPD−CPDyl addition or the CPDyl−CPDyl recombination pathway. Arguing that the first aromatic ring is most likely formed by reactions of two propargyl radicals rather than acetylene addition to *i*-C_4H_3 or *i*-C_4H_5, Miller and Melius[48] pointed out that the resonantly stabilized free radicals form very weak bonds with stable molecules and the addition complexes in such cases do not readily support rearrangement. By comparing the reactivity of resonantly stabilized free radicals and ordinary free radicals with molecular oxygen, one finds that the propargyl + O_2 rate coefficient at 1500 K is $\sim 10^{-14}$ cm^3 $molecule^{-1}$ s^{-1}, whereas that for vinyl + O_2 is $\sim 10^{-11}$ cm^3 $molecule^{-1}$ s^{-1}, more than a 2-order-of-magnitude difference.[49] The radical−radical reactions can occur at much higher rates than the radical−molecule reactions. In addition, the bond formed in the initial adduct of these reactions is expected to be much stronger than that of the radical−molecule reactions, thus providing greater opportunity for rearrangement and cyclization. For instance, the initial CPD−CPDyl adduct I1 lies only 8.71 kcal/mol below the reactants, while the CPDyl−CPDyl adduct C1 lies 39.46 kcal/mol below the reactants. However, in a hydrogen-rich environment I1 can readily undergo H abstraction to form C1 or D1. Besides, the energy barrier for I1 to decompose to CPD and CPDyl is 20.19 kcal/mol, which is likely to give I1 lifetime long enough for rearrangement as in the radical−molecule pathways proposed for the formation of indene and benzene.

5. Conclusions

In this paper, new reaction pathways for the formation of benzene, indene, and naphthalene are investigated for the CPD−CPDyl system, using the density functional level of theory. The kinetic mechanisms identified for the pyrolysis of CPD include intramolecular addition and C−H bond β-scission for the production of indene and naphthalene. New mechanisms that involve the C−C bond β-scission reaction are identified for the production of benzene, fulvene, and naphthalene.

The formation of other aromatic compounds observed in the experiments such as toluene, styrene, fluorene, phenanthrene, and anthracene was also explained by subsequent reactions of smaller aromatic compounds, for instance, benzene and indene. Rate constants for the first step of the pathways were calculated using the transition-state theory, which show that at low temperatures the yield of indene is the largest among the three while at high temperatures benzene tends to dominate, in agreement with the experiments. In a hydrogen-rich environment, H abstraction reactions by H atoms are considered, and they greatly improve the formation rate of naphthalene.

The computational results obtained in this paper provide information for further investigation of the importance of the cyclopentadienyl moieties in the growth of PAH, and additional studies that involve the use of a detailed kinetic mechanism for the formation of aromatics in a plug flow reactor have been already planned.

Acknowledgment. This research is funded by the National Science Foundation, Collaborative Proposal (CTS-0210061).

The calculations presented in this paper were carried out at the Utah Center for High Performance Computing, University of Utah that is acknowledged for computer time support.

Supporting Information Available: Cartesian coordinates of the new transition structure from F3 to F4 in pathway R6. This material is available free of charge via the Internet at http://pubs.acs.org.

References and Notes

(1) Benish, T. G.; Lafleur, A. L.; Taghizadeh, K.; Howard, J. B. *Proc. Combust. Inst.* **1996**, *26*, 2319.
(2) Lafleur, A. L.; Howard, J. B.; Taghizadeh, K.; Plummer, E. F.; Scott, L. T.; Necula, A.; Swallow, K. C. *J. Phys. Chem.* **1996**, *100*, 17421.
(3) Durant, J. L.; Busby, W. F.; Lafleur, A. L.; Penman, B. W.; Crespi, C. L. *Mutat. Res.* **1996**, *371*, 123.
(4) Durant, J. L.; Lafleur, A. L.; Busby, W. F.; Donhoffner, L. L.; Penman, B. W.; Crespi, C. L. *Mutat. Res.* **1999**, *446*, 1.
(5) Frenklach, M.; Clary, D. W.; Gardiner, W. C.; Stein, S. E. *Proc. Combust. Inst.* **1985**, *20*, 887.
(6) Frenklach, M.; Clary, D. W.; Yuan, T.; Gardiner, W. C.; Stein, S. E. *Combust. Sci. Technol.* **1986**, *50*, 79.
(7) Frenklach, M.; Clary, D. W.; Gardiner, W. C.; Stein, S. E. *Proc. Combust. Inst.* **1987**, *21* 1067.
(8) Frenklach, M.; Warnatz, J. *Combust. Sci. Technol.* **1987**, *51*, 265.
(9) Melius, C. F.; Colvin, M. E.; Marinov, N. M.; Pitz, W. J.; Senkan, S. M. *Proc. Combust. Inst.* **1996**, *26*, 685.
(10) Castaldi, M. J.; Marinov, N. M.; Melius, C. F.; Huang, J.; Senkan, S. M.; Pitz, W. J.; Westbrook, C. K. *Proc. Combust. Inst.* **1996**, *26*, 693.
(11) Colket, M. B.; Seery, D. J. *Proc. Combust. Inst.* **1994**, *25*, 883.
(12) Pope, C. J.; Miller, J. A. *Proc. Combust. Inst.* **2000**, *28*, 1519.
(13) McEnally, C. S.; Pfefferle, L. D. *Proc. Combust. Inst.* **2000**, *28*, 2569.
(14) Lindstedt, P.; Maurice, L.; Meyer, M. *Faraday Discuss.* **2001**, *119*, 409.
(15) Frenklach, M.; Taki, S.; Durgaprasad, M. B.; Matula, R. A. *Combust. Flame* **1983**, *54*, 81.
(16) Frenklach, M. *Phys. Chem. Chem. Phys.* **2002**, *4* (11), 2028.
(17) McEnally, C. S.; Pfefferle, L. D. *Combust. Sci. Technol.* **1998**, *131*, 323.
(18) Scott, L. T.; Roelofs, N. H. *J. Am. Chem. Soc.* **1987**, *109*, 5461.
(19) Howard, J. B.; Longwell, J. P.; Marr, J. A.; Pope, C. J.; Busby, W. F., Jr.; Lafleur, A. L.; Taghizadeh, K. *Combust. Flame* **1995**, *101*, 262.
(20) DasGupta, A.; DasGupta, N. K. *Can. J. Chem.* **1976**, *54*, 3227.
(21) Jenneskens, L. W.; Sarobe, M.; Zwikker, J. W. *Pure Appl. Chem.* **1996**, *68*, 219.
(22) Lu, M.; Mulholland, J. A. *Chemosphere* **2001**, *42*, 625.
(23) Mulholland, J. A.; Lu, M.; Kim, D.-H. *Proc. Combust. Inst.* **2000**, *28*, 2593.
(24) Kim, D. Y.; Mulholland, J. A.; Wang, D.; Violi, A. *Combust. Flame*, submitted for publication, 2005.
(25) D'Anna, A.; Violi, A. *Proc. Combust. Inst.* **1998**, *27*, 425.
(26) Violi, A.; Sarofim, A. F.; Truong, T. N. *Combust. Flame* **2001**, *126*, 1506.
(27) Violi, A.; Sarofim, A. F.; Truong, T. N. *Combust. Sci. Technol.* **2002**, *174* (11−12), 205.
(28) Becke, A. D. *J. Chem. Phys.* **1992**, *96*, 2155; **1992**, *97*, 9173; **1993**, *98*, 5648.
(29) Lee, C.; Yang, W.; Parr, R. G. *Phys. Rev. B* **1988**, *37*, 785.
(30) Hehre, W.; Radom, L.; Schleyer, P. R.; Pople, J. A. *Ab initio Molecular Orbital Theory*; Wiley: New York, 1986.
(31) Frisch, M. J.; Trucks, G. W.; Schlegel, H. B.; Scuseria, G. E.; Robb, M. A.; Cheeseman, J. R.; Montgomery, J. A., Jr.; Vreven, T.; Kudin, K. N.; Burant, J. C.; Millam, J. M.; Iyengar, S. S.; Tomasi, J.; Barone, V.; Mennucci, B.; Cossi, M.; Scalmani, G.; Rega, N.; Petersson, G. A.; Nakatsuji, H.; Hada, M.; Ehara, M.; Toyota, K.; Fukuda, R.; Hasegawa, J.; Ishida, M.; Nakajima, T.; Honda, Y.; Kitao, O.; Nakai, H.; Klene, M.; Li, X.; Knox, J. E.; Hratchian, H. P.; Cross, J. B.; Bakken, V.; Adamo, C.; Jaramillo, J.; Gomperts, R.; Stratmann, R. E.; Yazyev, O.; Austin, A. J.; Cammi, R.; Pomelli, C.; Ochterski, J. W.; Ayala, P. Y.; Morokuma, K.; Voth, G. A.; Salvador, P.; Dannenberg, J. J.; Zakrzewski, V. G.; Dapprich, S.; Daniels, A. D.; Strain, M. C.; Farkas, O.; Malick, D. K.; Rabuck, A. D.; Raghavachari, K.; Foresman, J. B.; Ortiz, J. V.; Cui, Q.; Baboul, A. G.; Clifford, S.; Cioslowski, J.; Stefanov, B. B.; Liu, G.; Liashenko, A.; Piskorz, P.; Komaromi, I.; Martin, R. L.; Fox, D. J.; Keith, T.; Al-Laham, M. A.; Peng, C. Y.; Nanayakkara, A.; Challacombe, M.; Gill, P. M. W.; Johnson, B.; Chen, W.; Wong, M. W.; Gonzalez, C.; Pople, J. A. *Gaussian 03*, revision C.01; Gaussian, Inc.: Wallingford, CT, 2004.
(32) Banisaukas, J.; Szczepanski, J.; Eyler, J.; Vala, M.; Hirata, S.; Head-Gordon, M.; Oomens, J.; Meijer, G.; Helden, G. V. *J. Phys. Chem. A* **2003**, *107*, 782.
(33) Ducan, W. T.; Bell, R. L.; Truong, T. N. *J. Comput. Chem.* **1998**, *19*, 1039.
(34) Truong, T. N.; Truhlar, D. G. *J. Chem. Phys.* **1990**, *93*, 1761.
(35) Melius, C. F.; Miller, J. A.; Evleth, E. M. *Proc. Combust. Inst.* **1992**, *24*, 621.
(36) Madden, L. K.; Mebel, A. M.; Lin, M. C.; Melius, C. F. *J. Phys. Org. Chem.* **1996**, *9*, 801.
(37) Gaynor, B. J.; Gilbert, R. G.; King, K. D.; Harman, P. J. *Aust. J. Chem.* **1981**, *34*, 449.
(38) Miller, J. A.; Klippenstein, S. J. *J. Phys. Chem. A* **2003**, *107*, 7783.
(39) Merz, K. M., Jr.; Scott, L. T. *J. Chem. Soc., Chem. Commun.* **1993**, 412.
(40) Violi, A.; Truong, T. N.; Sarofim, A. F. *J. Phys. Chem. A* **2004**, *108*, 4846.
(41) Truong, T. N.; Duncan, W. *J. Chem. Phys.* **1994**, *101*, 7408.
(42) Mebel, A. M.; Lin, M. C.; Yu, T.; Morokuma, K. *J. Phys. Chem. A* **1997**, *101*, 3189.
(43) Richter, H.; Benish, T. G.; Mazyar, O. A.; Green, W. H.; Howard, J. B. *Proc. Combust. Inst.* **2000**, *28*, 2609.
(44) Chang, A. Y.; Bozzelli, J. W.; Dean, A. M. *Z. Phys. Chem.* **2000**, *214*, 1533.
(45) Tokmakov, I. V.; Park, J.; Gheyas, S.; Lin, M. C. *J. Phys. Chem. A* **1999**, *103*, 3636.
(46) Braun-Unkhoff, M.; Frank, P.; Just, Th. *Proc. Combust. Inst.* **1988**, *22*, 1053.
(47) Marinov, N. M.; Castaldi, M. J.; Melius, C. F.; Tsang, W. *Combust. Sci. Technol.* **1997**, *128*, 295.
(48) Miller, J. A.; Melius, C. F. *Combust. Flame* **1992**, *91*, 21.
(49) Miller, J. A.; Pilling, M. J.; Troe, J. *Proc. Combust. Inst.* **2005**, *30*, 43.